PALLADIUM, A PROGRAM TO MODEL THE CHROMATOGRAPHIC SEPARATION OF THE PLATINUM-GROUP ELEMENTS, BASE METALS AND SULFUR IN A SOLIDIFYING PILE OF IGNEOUS CRYSTALS

ALAN E. BOUDREAU[§]

*Division of Earth and Ocean Sciences, Nicholas School of the Environment and Earth Sciences,
Duke University, Box 90227, Durham, North Carolina 27707, U.S.A.*

ABSTRACT

The formation of platinum-group-element (PGE) deposits in layered intrusions involves an interplay of sulfide saturation and modifications that might be caused by migrating silicate liquid and volatile fluid. The program PALLADIUM has been written to illustrate the chromatographic effects occurring in a pile of igneous crystals + liquid in a fractionating magmatic system, with a pile of cumulates that is both growing in thickness while also undergoing compaction, solidification and possible separation and migration of a volatile fluid phase. The program links compaction-driven mass transport with conductive cooling and compositional evolution controlled by equilibrium partitioning between phases. The elements S, Pd, Ir, Cu and Ni are assumed to follow simple partitioning behavior among the potential phases that include immiscible sulfide liquid, silicate liquid, volatile fluid, and Pd metal. All other precipitated solids are included in the solid matrix. The initial composition of the magma, compaction parameters and other variables can be set by the user. Two examples involving the crystallization of a "dry" and a "wet" magma are presented to illustrate the utility of the program. Both cases illustrate how chromatographic and reaction effects can lead to chromatographic separation of the elements and the formation of metal alloys and other PGE-rich, S-poor phases beneath sulfide zones, as are observed in many PGE deposits. The principal difference between the "dry" magmatic precipitation of sulfide as a cotectic phase and those sulfides arising from fluid migration in a crystallizing "wet" pile of crystals is that the former cannot exceed cotectic proportions of sulfide unless there is preferential settling of sulfide, and the Pd metal zone is ephemeral. In contrast, the latter mechanism can produce sulfide-enriched zones in which sulfide abundance exceeds expected cotectic levels of saturation.

Keywords: platinum-group-element deposits, geochemical modeling, layered intrusion, geochemical program, PALLADIUM.

SOMMAIRE

La formation de gisements d'éléments du groupe du platine au sein des massifs stratiformes implique le concours d'une saturation en sulfures et des modifications qui pourraient être dues à la migration d'un liquide silicaté et d'une phase fluide. Le logiciel PALLADIUM a été conçu pour illustrer les effets chromatographiques attendus dans un empilement de cristaux ignés avec liquide interstitiel dans un système magmatique en cours de fractionnement, les cumulats étant sujets à une compaction, solidification, séparation et migration d'une phase volatile fluide tout en devenant plus épaisse. Le logiciel établit un lien entre le transfert de masse dû à la compaction d'une part, et le refroidissement conductif et l'évolution de la composition, régie selon les coefficients de partage à l'équilibre parmi les phases présentes. On suppose que les éléments S, Pd, Ir, Cu et Ni suivent les règles d'une répartition simple parmi les phases attendues, par exemple liquide immiscible sulfuré, liquide silicaté, phase volatile, et Pd pur. Tous les autres solides sont compris dans la matrice solide. Le choix de la composition initiale du magma, les paramètres régissant la compaction, et certains autres paramètres peut être laissé à l'utilisateur. Deux exemples impliquant la cristallisation d'un magma avec et sans H_2O servent à illustrer l'utilité du logiciel. Les deux cas illustrent la façon par laquelle les effets chromatographiques et réactionnels peuvent mener à une séparation des éléments et à la formation d'alliages et d'autres phases enrichies en éléments du groupe du platine et à faible teneur en soufre en dessous des zones à sulfures, comme c'est le cas dans plusieurs gisements. Dans un magma "sec", la précipitation magmatique d'un sulfure ne pourrait dépasser la proportion cotectique, à moins qu'il y ait extraction de la phase sulfurée par accumulation vers la base due à la gravité; il en résulte que la zone contenant le Pd métallique est éphémère. En revanche, la précipitation de sulfures aux dépens d'un magma contenant un peu de H_2O peut mener à des zones enrichies en sulfures en proportions qui dépassent les proportions cotectiques.

(Traduit par la Rédaction)

Mots-clés: gisements d'éléments du groupe du platine, modèles géochimiques, complexe intrusif stratiforme, logiciel géochimique, PALLADIUM.

[§]   *E-mail address*: boudreau@duke.edu

INTRODUCTION

In the ongoing debate between the proponents of magmatic and hydrothermal mechanisms for the formation of deposits of the platinum-group elements (PGE) in layered intrusions (*e.g.*, Barnes & Campbell 1988), it has become clear to me that all too commonly the discussion as to how metals might be concentrated by a volatile fluid phase is hindered by a lack of understanding of how such a process may work. In order to address this problem, I have written the computer program PALLADIUM to illustrate some of the phenomena that can occur in a crystal + liquid pile that is simultaneously undergoing growth by addition of crystals at the top of the pile, compaction, crystallization, and the eventual separation and migration of a volatile fluid phase.

An earlier version of this program was used to describe how PGE – base metal "offsets" can develop as an aqueous fluid separates and migrates up through a pile of crystals (Boudreau & Meurer 1999), although it was not distributed. This version includes more elements and phases and allows for element partitioning into a generalized solid matrix not included in the original version. The user can set a variety of physical and compositional parameters to investigate conditions favorable to ore-metal transport, chromatographic separation and reaction phenomena in a crystallizing and degassing layered intrusion.

DESCRIPTION OF THE PROGRAM

The program PALLADIUM is written in Microsoft Visual Basic 6© for the Windows© PC platform. The program allows for first-order geochemical modeling of concentrations of the elements Ni, Cu, Pd, Ir and S as well as H_2O in a crystallizing magma chamber. Phases that are included in the program (and the short-hand terminology used in this report) include silicate liquid (liquid), volatile aqueous fluid (fluid), sulfide liquid (sulfide), a solid matrix (matrix), and Pd metal. The solid matrix includes all possible phases not modeled separately, and can be considered to be a mixture of silicate, oxide, and other minerals. The modeled elements are assumed to follow simple equilibrium-partitioning behavior into these phases.

A simple phase-equilibration routine is coupled with standard diffusion and advection one-dimensional heat- and mass-transport equations. This program is general enough for users to specify a range of starting compositions of magma. The program allows calculation of reaction and chromatographic fronts as compaction-driven silicate liquid and fluid percolate through a porous solid matrix. The details of the program are much as described by Boudreau & Meurer (1999). Some of the processes of mass and thermal transport in a body of crystallizing magma modeled the program are illustrated in Figure 1.

The growth and compaction of the crystal + liquid pile generally follow the methodology of Shirley (1986).

The top of the pile is allowed to grow at some constant velocity by the addition of crystals with an initial porosity of 60%. The deposition of these crystals leads to differentiation of the remaining magma in the chamber by standard Raleigh fractionation. If sulfide or fluid are not already present in the initial magma, fractional crystallization can cause the magma to become saturated in these phases.

For compaction, the bottom is assumed closed to mass transfer and the overlying solid assemblage is allowed to collapse under its own weight. Compaction essentially follows Shirley's (1986) scheme using the equations of McKenzie (1984). For the purposes of this work, the more important equations are those that describe the compaction-driven velocities of solid matrix and liquid (symbols and values of fixed constants are defined in Table 1):

$$\left(\xi + \frac{4}{3}\eta\right)\left((1-f)\frac{\partial^2 V_s}{\partial z^2} - \frac{\partial f}{\partial z}\frac{\partial v}{\partial z}\right)$$
$$= \frac{\mu}{K_f} V_s + (1-f)(\rho_s - \rho_1)g \quad (1)$$

and

$$V_1 = -\frac{(1-f)}{f} V_s \quad (2)$$

TABLE 1. LIST OF SYMBOLS USED IN THE PROGRAM PALLADIUM

Symbol	Definition	Units	Value
a	Crystal radius	m	0.0003
C	Concentration	dimensionless	calculated
Cp	Heat capacity	$J\ K^{-1}\ kg^{-1}$	1000
D_{bulk}	Bulk distribution coefficient	dimensionless	calculated
f	Liquid fraction	dimensionless	calculated
g	Gravitational acceleration	$m\ s^{-2}$	9.8
ΔH_{cryst}	Heat of crystallization	$J\ kg^{-1}$	100,000
K_d^i	Distribution coefficient for element i	dimensionless	user-defined
K_f	Permeability of matrix	m^2	calculated
K_0	Permeability constant	dimensionless	user-defined
q	Heat	J	calculated
T	Temperature	K	calculated
t	Time	s	calculated
V_s, V_1	Velocity of solid matrix, liquid	$m\ s^{-1}$	calculated
X_i	Wt. fraction phase i	dimensionless	calculated
z	Vertical coordinate	m	calculated
κ	Thermal diffusivity	$m^2\ s^{-1}$	5×10^{-7}
μ	Viscosity of the liquid	Pa s	user-defined
η	Shear viscosity of solid matrix	Pa s	user-defined
ξ	Bulk viscosity of solid matrix	Pa s	user-defined
ρ_s, ρ_1	Density of solid matrix, liquid	$kg\ m^{-3}$	3,000, 2,700
Ψ	Mass crystallized	$kg\ m^{-3}$	calculated
*	Denotes characteristic value		

In equation 1, the first expression in parentheses on the left is the effective viscosity of the matrix and is the combination of the bulk and shear viscosities of the solid matrix; the effective viscosity is set by the user. The density difference between solid and liquid, $\rho_s - \rho_l$, is assumed fixed at 300 kg m^{-3}. The parameter K_f is the permeability of the matrix and, using the expressions of Shirley (1986), is taken to be a function of grain size and liquid fraction:

$$K_f = K_0 a^2 g(f) \qquad (3)$$

where

$$g(f) = \frac{f^3}{(1-f)^2} \qquad (4)$$

Much of the variation caused by changing fixed parameters such as the permeability constant K_0 and the effective viscosity of the solid can be expressed in the "characteristic" length and time scale for compaction,

as well as the characteristic velocity of the solid matrix (Shirley 1986):

$$z* = a\left(\frac{K_0\left(\xi + 4\eta/3\right)}{\mu}\right)^{\frac{1}{2}} \qquad (5)$$

$$t* = \left(\frac{\mu\left(\xi + 4\eta/3\right)}{K_0}\right)^{\frac{1}{2}} a^{-1} g^{-1} \left(\rho_s - \rho_l\right)^{-1} \qquad (6)$$

$$V* = \frac{z*}{t*} \qquad (7)$$

The characteristic velocity, $V*$, is used to scale the upward growth of the pile and to scale the velocity of the fluid in the pile, as described below. In the program, only the permeability constant, K_0, the viscosity of the liquid, μ, and the effective viscosity of the solid, $(\xi + 4\eta/3)$, can be changed by the user; the others are as listed in Table 1. As pointed out by Shirley (1986), K_0 and the
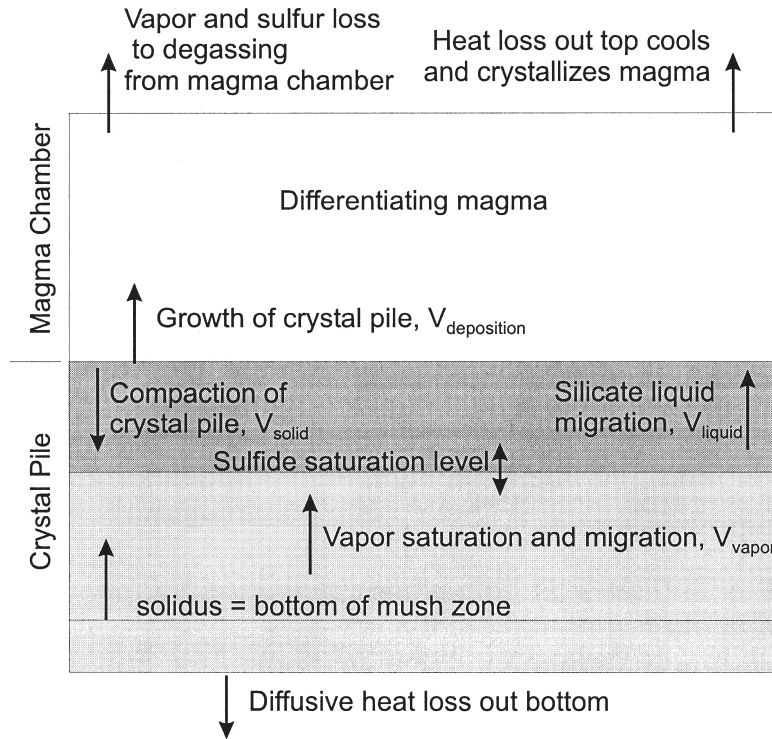

Fig. 1. Cartoon showing the fluxes modeled by the program PALLADIUM.

viscosity of the solid are the two more critical compaction-related parameters. Changing these variables, along with the rate of growth of the pile, allow one to model a thin or thick zone of compaction. However, any combination of the variables in Equations (6) and (7) that result in the same characteristic distance and time will have quantitatively the same compaction behavior. Thus, a clever choice of the three adjustable parameters to get the desired characteristic values allows one to model the effect of changing other parameters, such as the difference between density of solid and liquid, ($\rho_s - \rho_l$), or (as one reviewer wished), a change in the gravitational constant, g.

HEAT TRANSPORT

In the model, the compacting crystal + liquid pile can undergo additional crystallization because of cooling through the base, at a rate set by the user. Cooling at the base stops once the basal temperature reaches 500°C. The temperature of the fractionating liquid in the chamber above the pile is calculated as a linear function of the pile thickness, cooling from 1250°C at the start to 1000°C when the pile reaches the top of the chamber. Once the pile reaches the top of the chamber, the top of the pile cools at the same rate as does the base.

The evolution of temperature with time is governed by two parameters: a) thermal diffusion, and b) addition of heat from the latent heat of crystallization. The change in advective heat caused by compaction is ignored because compaction is largely thermally neutral: hot matrix moving down is approximately thermally balanced by cooler liquids moving up (unpublished results). An additional simplifying assumption is made that the heat capacities of the liquid, volatile fluid, and all matrix phases are equal. (Although this is a good approximation for the liquid and solid, it is less so for a fluid, but the latter is typically a volumetrically minor phase.) With these simplifications, the evolution of temperature can be expressed by a numerical analog of the following equation describing one-dimensional heat transport:

$$\frac{\partial T}{\partial t} = \kappa \frac{\partial^2 T}{\partial x^2} + \frac{\Delta H_{cryst}}{\rho C_p} \frac{\partial \Psi}{\partial t} \qquad (9)$$

where $\dfrac{\partial \Psi}{\partial t}$ is the change in the mass crystallized per unit volume with time. Values for the constants are listed in Table 1.

Heat loss from the crystal + liquid assemblage causes crystallization. The change in the amount of crystalline material can be expressed as a function of the gain or loss of heat, q, with time:

$$\frac{\partial \Psi}{\partial t} = \frac{\partial \Psi}{\partial q} \frac{\partial q}{\partial t} \qquad (10)$$

where $\dfrac{\partial \Psi}{\partial q}$ is the fraction crystallized per unit loss in heat, and $\dfrac{\partial q}{\partial t}$ is the heat transfer resulting from thermal diffusion. In the program, crystallization is modeled as a simple function of heat loss, such that

$$\frac{\partial \Psi}{\partial q} = \frac{1}{\Delta H_{cryst}} \qquad (11)$$

FLUID EVOLUTION, SULFIDE SATURATION AND ELEMENT TRANSPORT

The evolution of an aqueous fluid from the solidifying interstitial liquid used in the model is as proposed by Boudreau & McCallum (1992). The initial sulfur and H_2O contents of the silicate liquid are set by the user. For initial contents of H_2O, typical values might range from a low of about 0.2 wt.% for MORB-type liquids to in excess of 1.0 wt.% H_2O; this latter value represents a low end for H_2O contents in boninitic liquids (Sobolev & Chaussidon 1996) and is likely to be realistic for many high-Mg layered intrusion magmas (Boudreau *et al.* 1997). The silicate liquid is assumed to be fluid-saturated when the H_2O concentration reaches a user-defined value. For a basalt at 2 kbar, a typical value might be 5.0 wt.% H_2O (Holloway & Blank 1994).

Any fluid separating from the main body of magma above the pile is assumed to be lost from the system, along with any elements it contains. Any fluid that is exsolved in the pile of crystals is assumed to migrate up through the pile. In the pile, the mass of fluid that is evolved (as bubbles) in one space-step is allowed to migrate upward and re-equilibrate with each overlying space-step until it encounters fluid-undersaturated interstitial liquid. On encountering fluid-undersaturated liquid, the sulfur, metal and H_2O content of the fluid is added to the interstitial liquid in that zone. The top of the pile is not allowed to become vapor-saturated; any fluid reaching this level is assumed to have its mass of H_2O added to the mass of overlying magma. The velocity at which bubbles may rise through a compacting pile of crystals has not been addressed, as far as is known. Because of this, fluid velocity is generalized and is taken to be proportional to the characteristic compaction velocity; this proportionality constant is set by the user.

As summarized by Carroll & Webster (1994), sulfur solubility in natural basalts can range from <100 to >1000 ppm S, and is controlled largely by oxygen fugac-

ity, temperature, pressure, and Fe content of the liquid. Background bulk sulfur contents of cumulates conventionally interpreted to be sulfide-saturated at the time of their formation are on the order of a few hundred ppm (*e.g.*, Hoatson & Keays 1989). If these values represent cotectic proportions of sulfide separating from the magma, they imply that sulfur concentrations in the magma were of a similar order. This estimate reflects the fact that the magma precipitates sulfide to keep an approximately constant S concentration. In other words, the bulk precipitated assemblage and the magma will both have the same bulk S concentrations. This sulfide-saturation value is set by the user. At sulfide saturation, the sulfide phase is assumed to contain 0.40 wt. fraction sulfur. Once sulfide is present, it is assumed to move with the host matrix during compaction.

The partitioning of metals and S during fractional separation of a fluid is modeled as a local equilibrium process over small intervals of solidification. The S content of a sulfide-saturated aqueous fluid can be set by the user. Sulfur concentrations in a fluid along any given oxygen buffer are typically a strong positive function of temperature. Calculated values range from about 2.5 wt.% S at 900°C and 2 kbar based on fayalite – orthopyroxene – pyrrhotite – O – H – S fluid equilibria at QFM oxygen buffer (Barnes & Campbell 1988) to about 20 wt.% S at 1200°C and 1 kbar based on fayalite – magnetite – quartz – pyrrhotite – O – H – S fluid equilibria (Shi 1992). The maximum value that can be entered is 20 wt.%.

When the system is not saturated in sulfide, the partitioning of sulfur between fluid and liquid is calculated using a fluid/liquid partition coefficient equivalent to that of the sulfide-saturated fluid and liquid. For example, if at sulfide saturation the user-set values are such that the fluid contains 0.1 wt. fraction S, and the liquid, 0.001 wt. fraction S, the fluid/liquid partition coefficient for S for a sulfide-undersaturated condition would be calculated by the program as 0.1/0.001 = 100.0.

Finally, the element Pd is allowed to precipitate as a Pd metal if the concentration of Pd in the liquid exceeds a user-set saturation concentration. This phase might be thought of as a proxy for a PGE metal alloy or other PGE-rich, S-poor phases that may be found in layered intrusions.

The program's operation can be briefly summarized as follows. The user first enters all pertinent physical parameters for the composition of the initial magma, including the initial sulfur, H_2O and Pd content, partition coefficients for the various metals between sulfide and silicate liquids, fluid and silicate liquid, and silicate crystals and silicate liquid, and the saturation concentration for Pd metal. For compaction, the user enters values for the viscosity of the liquid and solid, the permeability constant K_0, and a velocity at which crystals are being deposited at the top of the pile, the latter a constant that calculates the growth rate of the pile as proportional to the characteristic compaction velocity

(Eq. 7). Miscellaneous parameters set by the user include height of the magma chamber, a proportionality constant for the velocity of the fluid phase (scaled by the characteristic velocity as described above), a cooling rate constant for cooling at the bottom of the pile, and limiting values for the liquid fraction, f, at which compaction and solidification are assumed complete (typically 0.01 and 0.001, respectively). Once all pertinent values have been entered, they can be saved to a text file.

After the initial parameters have been entered, the user starts the simulation. The pile grows by the addition of crystals at the top. Simultaneous cooling at the base of the pile and compaction lead to both an evolving interstitial liquid and a reduction of the liquid fraction. At each time and space step, the velocities of the solid, liquid and fluid are calculated. Change in bulk concentrations and phase proportions are calculated using numerical analogs to the above partial differential equations and standard advective mass-transfer and thermal diffusion expressions (*e.g.*, von Rosenberg 1969). Once the new bulk composition and phase proportions are calculated, new equilibrium concentrations of the phases are calculated from the following expression:

$$C = \frac{C_{bulk}}{D_{bulk} + f\left(1 - D_{bulk}\right)} \qquad (12)$$

where

$$D_{bulk} = \Sigma \, X_i \, K_d^i \qquad (13)$$

The interplay of crystallization, degassing and fluid migration leads to a variety of scenarios where sulfide and metals are precipitated at one stratigraphic level only to be later remobilized. The program allows one to follow the evolution of the bulk composition or that of individual phases (*e.g.*, fluid or sulfide composition) over time. The data at the end of any time step can be saved to a tab-delineated text file that can be easily imported into a spreadsheet.

LIMITATIONS AND POSSIBLE FUTURE IMPROVEMENTS TO THE PROGRAM

As noted above, the purpose of the program PALLADIUM is to allow first-order insights into the interplay of crystallization and degassing behavior on ore-metal distribution in layered intrusions. For example, the program does not allow preferential settling of sulfide, nor does it consider "R-ratio" variations in which sulfide may equilibrate with a variable mass of magma (Campbell *et al.* 1983). However, the simple Raleigh fractionation model used by the program means that the R-ratio is always at its maximum possible value. For example, if at any given time-step the amount of

crystalline material added to the pile is equal to 1.0 wt.% of the remaining mass of magma, and sulfide comprises 0.1 wt.% of the fractionated assemblage, then the R ratio would be $1/(0.01*0.001) = 10^5$. This "maximum R-ratio" is calculated by the program for sulfide added to the crystal pile at each time-step once the magma reaches saturation in a sulfide.

In addition, the program uses a fixed number of space steps (currently 1,000). Thus, for a column 1.0 km high, the spatial resolution would be 1.0 m. All concentrations would be averages over this thickness. For elements that can form sharp chromatographic concentration fronts, such as the PGE, the elements may be strongly concentrated over smaller length-scales and thus concentrated in a single space-step.

There are a number of areas where the program could be improved. For example, one could add routines that consider mixed CO_2–H_2O fluid and their different solubilities in a silicate liquid (*e.g.*, Holloway & Blank 1994). Similarly, one could add a sulfur speciation and concentration in the fluid as a function of temperature based on the equilibria mentioned above. One could also include chlorine as an additional trace element. Chlorine is a potentially important agent for the transport of the PGE (*e.g,*, Sassani & Shock 1990). Furthermore, partitioning between silicate liquid and fluid is, for many metals, an exponential function of Cl concentration in the fluid phase (*e.g.*, Holland 1972). Also, one could include other factors that control sulfide solubility such as Fe content of the liquid, oxygen fugacity, temperature, and pressure (*e.g.*, Carroll & Webster 1994).

Finally, one may wish to model different elements that those used in the program. These can be accommodated with the existing program: one simply enters relevant partition coefficients, *etc.*, for the desired element in place of those for, say, Ni, and remember that Ni is now just a proxy name for the desired element.

ILLUSTRATIONS OF THE PROGRAM'S OUTPUT

To illustrate the program, two sample cases are shown here. In the first case, the magma is dry, and crystallization and growth of the crystal pile lead to eventual saturation in sulfide. In the second case, the initial magma contains some H_2O that eventually separates as an aqueous fluid phase from crystallizing interstitial liquid. Values of all pertinent user-input parameters, including sulfide/liquid partition coefficients for Ni, Cu, Pd and Ir, are listed in Table 2.

For the PGE, such as Pt and Pd, measured solubility in silicate liquids is on the order of a few tens of ppb at oxygen fugacity around QFM to at most a few hundred ppb at higher oxygen fugacities (*e.g.*, Borisov *et al.* 1994, Borisov & Palme 1997), although in some cases their samples were Fe-free. In contrast, their solubility in a Cl-bearing aqueous fluid is probably highly variable but estimated to be on the order of a few ppm to a few tens of ppm (*e.g.*, Sassani & Shock 1990, Hsu *et al.*

1991, Ballhaus *et al.* 1994). On that basis, a fluid/liquid distribution coefficient for Pd on the order of 10–100 seems reasonable. However, it should be realized that Pd solubilities in either liquids or fluids at magmatic temperatures are not well known.

The solubility of Ir in a silicate liquid is on the order of hundreds of ppb (Peach & Mathez 1996). The solubility of Ir in a fluid is assumed to be similar to that of Pd, but it is also assumed to have significant partitioning into the solid matrix. Whereas there is increasing consensus that Ir is not likely to go into silicate minerals in any significant amount, the matrix can be composed of some fraction of oxides (consider a magma precipitating a chromitiferous pyroxenite, for example), which might incorporate some of this element (*e.g.*, Peach & Mathez 1996).

Copper is not likely to be a trace component in any sulfide phase, although it is treated by the program to follow simple partitioning behavior. A value of 150 is used for Cu partition coefficient between fluid and liquid; this value is used so that the sulfide phase dissolves approximately congruently.

The results discussed below do not qualitatively change for modest variations in any of these parameters or, for some parameters, even order-of-magnitude variations. In some instances, the effect of a change in one aspect of the model (*e.g.*, using lower solubility for an element in a degassing fluid) may be offset by other

TABLE 2. USER-SUPPLIED VALUES USED FOR THE TWO EXAMPLE RUNS DISCUSSED IN THE TEXT

	Case 1	Case 2
$C_0(H_2O)$ in initial magma	0.00	0.01
$C(H_2O)$ at fluid saturation	0.05	0.05
$C_0(S)$ in initial magma	0.00025	0.00025
$C(S)$ at sulfide saturation	0.0004	0.0004
$C_0(Pd)$ in initial magma	10 ppb	10 ppb
$C(Pd)$ Pd saturation in liquid	500 ppb	500 ppb
Partition coefficients for Pd:		
Fluid/Liquid	50	50
Sulfide/Liquid	10,000	10,000
Matrix/Liquid	0	0
Partition coefficients for Ir:		
Fluid/Liquid	50	50
Sulfide/Liquid	10,000	10,000
Matrix/Liquid	2	2
Partition coefficients for Cu:		
Fluid/Liquid	150	150
Sulfide/Liquid	700	700
Matrix/Liquid	0	0
Partition coefficients for Ni:		
Fluid/Liquid	50	50
Sulfide/Liquid	250	250
Matrix/Liquid	3	3
Compaction and miscellaneous parameters:		
Deposition velocity (scaled to V*)	0.50	0.50
Viscosity of liquid (Pa s)	10	10
Viscosity of matrix (solid) (Pa s)	5×10^{14}	5×10^{14}
Permeability constant, K_0	0.0015	0.0015
$C(S)$ in sulfide-saturated fluid	0.1	0.1
Chamber thickness (m)	1000	1000
V(fluid) multiplier (scaled to V*)	0.4	0.4
Cooling rate at bottom of pile (°C/yr)	-0.05	-0.5

variables (*e.g.*, higher concentrations of H_2O in the initial magma).

Case 1: dry magma

The initial magma is dry and sulfide-undersaturated. The evolution of compositional profiles with time is shown in Figure 2. Early in the crystallization, the concentration of the strictly chalcophile elements Pd, Cu, and S within the pile is controlled by the amount of interstitial liquid. Because of this distribution, compaction initially causes their bulk concentrations to decrease with depth, even though crystallization is increasing their concentrations in the interstitial liquid. The loss of these elements from the pile is halted once the cooling interstitial liquid reaches saturation in sulfide, producing the region of sulfide-saturated interstitial liquid labeled "Lower Sulfide zone" in Figure 2. The amount of sulfide and chalcophile elements in this zone is mainly

controlled by the amount of interstitial liquid present at the time the liquid reaches sulfide saturation. Although not evident in Figure 2, ongoing compaction of the sulfide + matrix assemblage causes a very modest increase in modal sulfide, and the bulk concentration of the ore elements as the depleted liquid is lost.

In contrast, those elements that partition into the solid matrix as well as sulfide, such as Ir, are progressively fractionated from the magma as the pile continues to grow. Sulfur concentration in the magma increases by fractional crystallization until the magma becomes saturated in sulfide at 450 m. This region is labeled "Upper Sulfide zone" in Figure 2. The cotectic proportion of sulfide at and above the "sulfide-in" level is 0.1 wt.% of the total precipitated assemblage. Further crystallization leads to additional precipitation of sulfide with height, and the PGE begin to show stronger fractionation-induced trends with height in the pile.
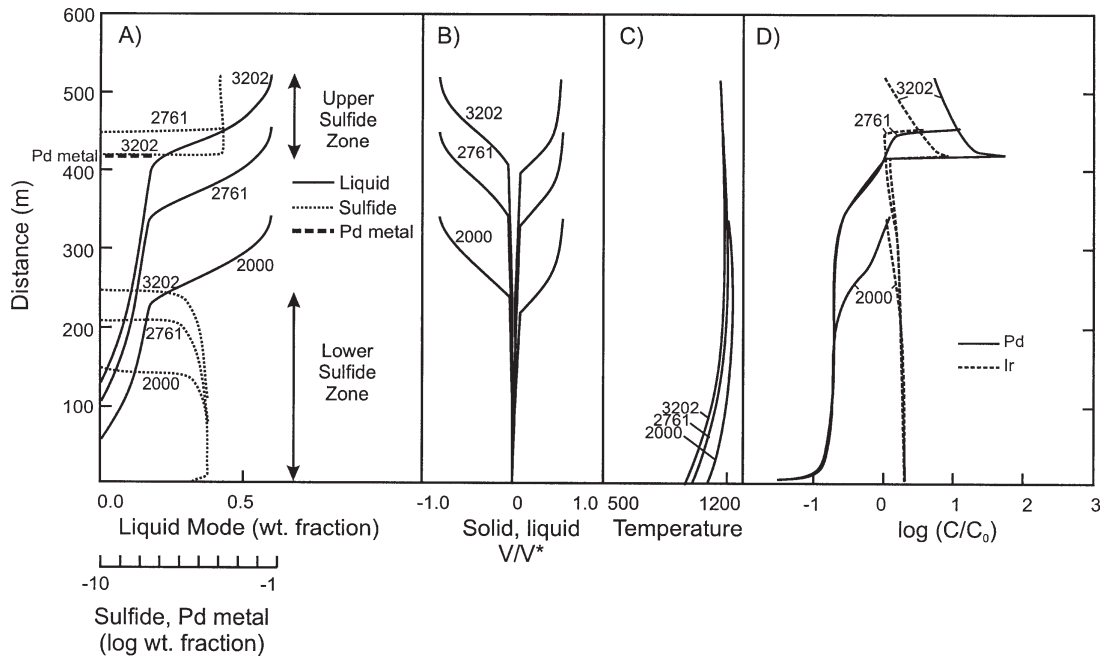

FIG. 2. Case 1: "dry" magma crystallization; user-supplied variables as listed in Table 2. Profiles are shown in the growing pile at the three time steps of 2000, 2761, and 3202 years. Initial thickness of the magma chamber is 1 km. A) Wt. fraction liquid (solid line, linear scale), sulfide (fine dashed line, log scale), and Pd metal (heavy dashed, labeled, log scale, x). B) Velocities of solid matrix and interstitial liquid, scaled to the characteristic velocity (Eq. 7). C) Temperature. D) Bulk element concentration normalized to initial concentrations of Pd (solid line) and Ir (dashed line) in the magma. Region marked "Lower Sulfide Zone" is sulfide precipitated from solidifying interstitial liquid, the top of which moves up with time owing to upward-migrating solidification front. Region marked "Upper Sulfide Zone" is sulfide precipitated once the magma in the chamber reaches sulfide saturation, the bottom of which moves down with time owing to compaction. With additional time, the two sulfide zones will merge and the Pd metal zone shown at 3202 yrs disappears (not shown). See text for additional discussion.

Compaction leads to four significant effects on the originally precipitated sulfide and element concentrations in the upper sulfide zone at the "sulfide-in" point where the magma first reached sulfide saturation. First, compaction causes the stratigraphic level of the "sulfide-in" horizon to move down over time with the compacting matrix. Between 2761 and 3202 yrs, the sulfide-in level has dropped about 30 m.

Second, because the immediately underlying interstitial liquid is not yet sulfide-saturated (a consequence of being far from the cooling boundary at the base of the pile) and thus has not lost its Pd concentration, there is a modest increase in the PGE content in the initially precipitated sulfide over time. This occurs as these elements are scavenged from the upward moving liquid by the sulfide as these liquids move through the sulfide-in front.

Third, as compaction continues, the liquids initially entering the sulfide-in front are increasingly undersaturated in sulfide as less-evolved, S-poor interstitial liquid from progressively deeper levels migrates upward over time. As a consequence, sulfide is increasingly resorbed at the sulfide-in front as these liquids dissolve sulfide to become sulfide-saturated. In effect, the sulfide-in boundary does not move down with the same velocity as the surrounding solid matrix assemblage.

Fourth, as a consequence of these first three processes, the concentration of Pd in the interstitial liquid at the resorption front in the upper sulfide zone increases over time. This increase occurs because once the sulfide is completely resorbed, the liquid is the next best host for the Pd. Eventually, the Pd concentration in the liquid at the sulfide-dissolution front exceeds the saturation point of Pd metal in the liquid (taken here as 500 ppb), and Pd metal precipitates.

The profile after 3202 years is characterized by a peak in the bulk Pd concentration at and below the sulfide-in front, with much of the Pd occurring in a metalliferous zone below the first appearance of "cumulus" sulfide. Sulfide concentrations never exceed expected cotectic proportions of 0.1 wt.% of the precipitated assemblage. This limit follows from the requirement of fixed concentration of sulfur in the liquid at sulfide saturation; the precipitated assemblage contains the same bulk concentration of S as the interstitial liquid, so that the liquid remains at constant S concentration.

The enrichment in PGE at the sulfide-in front continues, and the thin Pd metal zone only continues to be present as long as the interstitial liquid below the sulfide-in level remains sulfide-undersaturated. Although not shown in Figure 2, the Pd metal zone is ephemeral; eventually, the lower sulfide zone merges with the upper sulfide zone, the Pd metal redissolves in the new interstitial sulfide, and the Pd metal zone disappears.

For the case where cooling of the column results in sulfide saturation in the interstitial liquid prior to extensive compaction, the interstitial liquid is rapidly depleted in the PGE. Chromatographic enrichments in this situation would be considerably less important.

Case 2: "wet" magma

The initial magma in the case of a "wet" magma is similar as for Case 1, but it now has 1.0 wt.% H_2O. Compositional profiles as they develop over time are shown in Figure 3, with a detail of the profile at 2621 years shown in Figure 4. As for Case 1, growth of the crystal pile leads to eventual saturation in sulfide, although the time intervals of Figure 3 show the system prior to sulfide saturation in the magma. Also as for Case 1, the interstitial liquid in the lower part of the chamber also eventually becomes sulfide-saturated with cooling at the base.

In addition, however, crystallization of the interstitial liquid leads to enrichment of the liquid in H_2O and eventual saturation in an aqueous fluid. As this fluid moves upward, it carries with it sulfur and ore elements. The fluid continues to move upward until it encounters less evolved, volatile-poor interstitial liquid that is not fluid-saturated, at which point the fluid dissolves into the interstitial liquid. The addition of sulfur to the interstitial liquid by the fluid leads to significant additional precipitation of sulfide above what would precipitate by cooling interstitial liquid alone (Fig. 4). Thus, unlike in Case 1, the amount of sulfide precipitated can exceed expected cotectic proportions because of this fluid-added sulfur. This process continues until the interstitial liquid becomes fluid-saturated, at which point the local environment begins to lose sulfur to the separating fluid, and sulfur is again transported upward with the fluid.

Note that although Pd and Ir have the same model solubility in terms of fluid/liquid partitioning, fluid transport of Ir and Ni is rather minor, and the bulk-rock Pd:Ir and Pd:Ni ratios at the metal front increase with time. This happens because unlike Pd and Cu, Ir and Ni have been set to have significant partitioning into the non-sulfide solid matrix, and hence degassing of a small mass of fluid does not strongly change their bulk concentration.

As for Case 1, Pd is concentrated at (and just below) the sulfide-in front, and over time, Pd concentrations increase such that a Pd metal zone develops just below the sulfide-in front, as shown at 2621 yrs. The main difference is that fluid transport leads to a higher modal abundance of sulfide at the sulfide-in front, and this abundance increases with time. Also, unlike in Case 1, where compaction moves the sulfide-in front downward, the upward migration of fluid causes the S-enriched zone to move upward with time. In addition, the Pd metal front is not ephemeral because sulfur is effectively removed from the underlying interstitial liquid by the exsolving fluid.

The migrating sulfide-in front also produces characteristic offsets in the maximum concentrations of the various elements (Fig. 4). At 2621 years, the peak in Pd concentration is two meters beneath the peak in Cu concentration.

Although not shown, the upward moving metal front will merge in time with the "sulfide-in" front, at the level where the fractionating magma reaches sulfide saturation. The metal front continues to move upward, however, and the "sulfide-in" point is characterized by a thin zone of higher-than-cotectic proportions of sulfide overlying a Pd metal zone.

Comparison with rocks

For both Case 1 and Case 2, the model results have a number of parallels with observed ore-element distributions in rocks. For example, Oberthür *et al.* (2002) described S-poor PGE-rich minerals and alloys occurring below the main accumulations of sulfide in the Great Dyke. It should be noted that in real rocks, other "insoluble" PGE minerals, such as PGE-arsenides or PGE-bearing alloys, may take the place of the Pd metal precipitated in the model. What these models demonstrate is that unusually high levels of the PGE and unusually low concentrations of S in the interstitial liquid concentrations can develop within the pile that would not be otherwise reasonable to find in the parent magmas.

Other cases can be modeled in which the fluid transport of ore elements reaches the top of the pile. In this case, there can be a collapse of the chromatographic fronts, such that the ore-element concentration profiles all peak at the top of the crystal pile.

CONCLUSIONS

The model results illustrate that characteristic compositional "offsets" of the various ore-element concentrations and trace PGE-bearing minerals (*e.g.,*
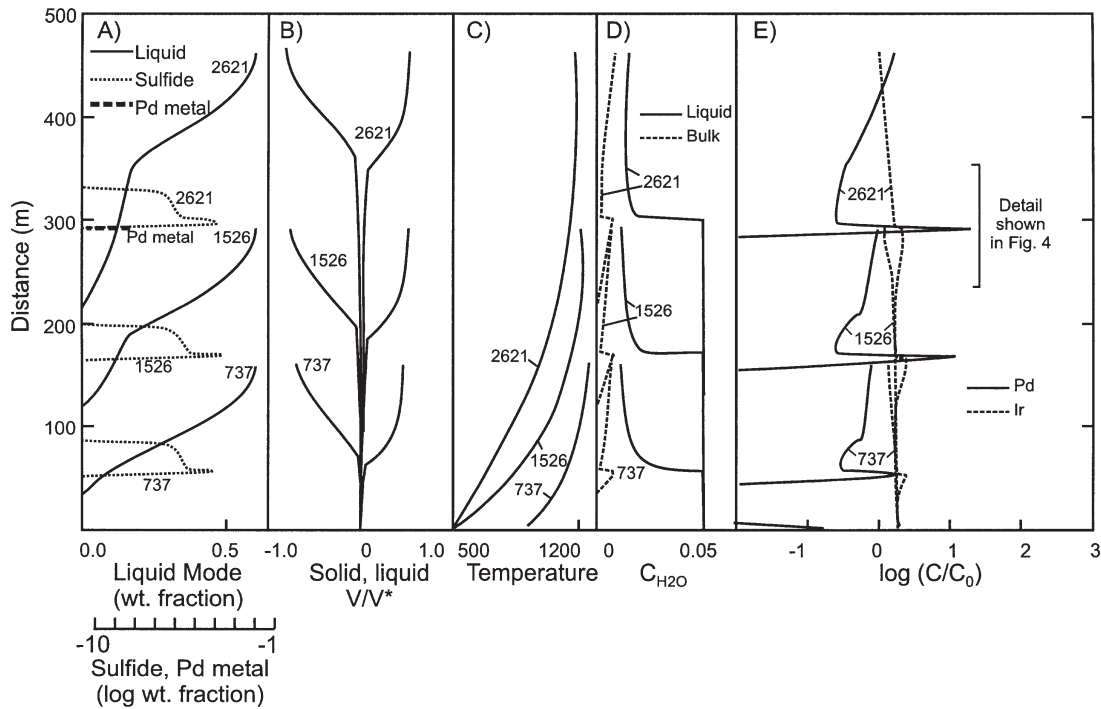

FIG. 3. Case 2: "wet" magma crystallization; user-supplied variables as listed in Table 2. Profiles are shown in the growing pile at time steps of 737, 1526, and 2621 years. Similar to case 1, but the initial H_2O content in the magma is now 1 wt.%, and the cooling rate at the bottom is twice as fast. A) Wt. fraction liquid (solid line, linear scale), sulfide (fine dashed line, log scale) and Pd metal (heavy dashed, labeled "Pd metal", log scale). B) Velocities of solid matrix and interstitial liquid velocities, scaled to the characteristic velocity (Eq. 7). C) Temperature. D) Concentration of H_2O in liquid, (solid line) and bulk H_2O content, , (dashed line) . E) Bulk element concentration normalized to initial concentrations of Pd (solid line) and Ir (dashed line) in the magma. A zone of increasing modal sulfide and Pd/Ir enrichment moves upward over time, and immediately below which eventually develops a zone of Pd metal, as shown in the 2621 year profile. See text for additional discussion.
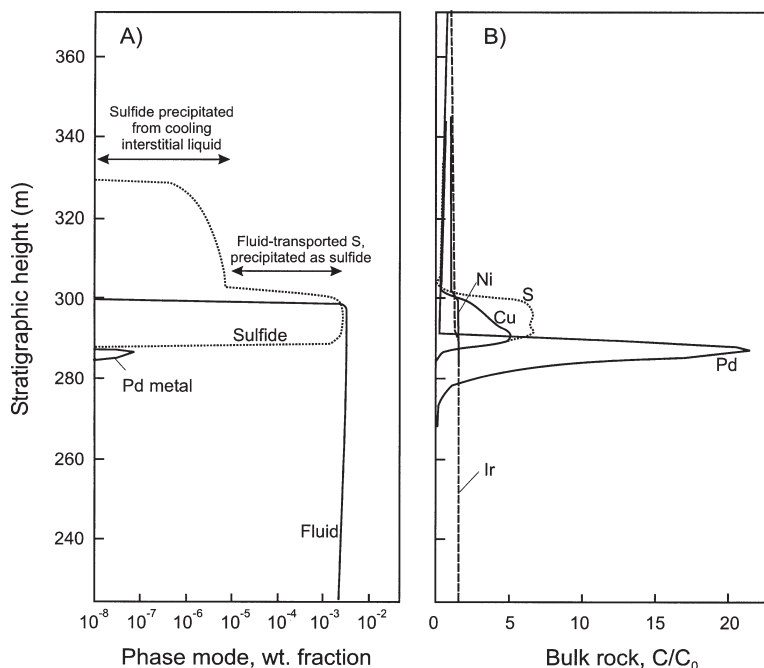
FIG. 4. Detail of the Case 2 run at 2621 years. A) Wt. fraction of fluid, sulfide and Pd metal as a function of stratigraphic height. B) Bulk-rock concentration of the elements S, Pd, Ir, Cu, and Ni, all normalized to initial composition of the magma. In A), the peak in sulfide mode labeled "Fluid-transported S, precipitated as sulfide" is that portion of the sulfide that is the result of fluid transport of sulfur. It migrates to higher stratigraphic levels with time. The portion of the sulfide mode labeled "Sulfide precipitated from cooling interstitial liquid" is the sulfide that results from the cooling and crystallizing interstitial silicate liquid. It also migrates upward with time. Note also the Pd metal zone that develops stratigraphically below the sulfide-bearing zone.

Prendergast & Wilson 1989, Barnes 1993, Bird *et al.* 1995, Anderson *et al.* 1998, Oberthür *et al.* 2002) can be produced by chromatographic separations by both strictly magmatic and hydromagmatic mechanisms within a compacting pile. In the model, the main distinguishing feature between the two mechanisms is that the hydromagmatic enrichments allows for the formation of zones with high bulk abundances of sulfur and sulfide. In contrast, magmatic precipitation of sulfide requires S enrichment in the silicate liquid by crystallization of silicate minerals, and thus never increases above the nominal cotectic proportions. Formation of magmatic sulfide modes above cotectic proportions would require preferential settling of sulfide, which must be justified on the basis of geological observations. In contrast, hydrothermal mobilization and concentration are most effective where bulk sulfur contents are low, prior to the level at which the magma reaches sulfide saturation.

Finally, the model suggests that the presence of PGE alloys and other insoluble PGE-rich phases can easily form as the result of loss of S to migrating sulfide-undersaturated fluid or silicate liquid; these phases can precipitate once the sulfide host has been resorbed. For the fluid-free models, the Pd zones may be ephemeral, as Pd metal will readily redissolve into sulfide once the interstitial liquid reaches sulfide saturation.

The program PALLADIUM and instructions for its use can be downloaded for the author's web site at www.env.duke.edu. Comments, bug reports and suggestions for improvement are always welcome and can be sent to the author at boudreau@duke.edu.

REFERENCES

ANDERSEN, J.C.Ø., RASMUSSEN, H., NIELSEN, T.F.D. & RØNSBO, J.G. (1998): The triple group and the Platinova gold and palladium reefs in the Skaergaard intrusion: stratigraphic and petrographic relations. *Econ. Geol.* **93**, 488-509.

BALLHAUS, C., RYAN, C.G., MERNAGH, T.P. & GREEN, D.H. (1994): The partitioning of Fe, Ni, Cu, Pt and Au between sulfide, metal and fluid phases: a pilot study. *Geochim. Cosmochim. Acta* **58**, 811-826.

BARNES, S.J. (1993): Partitioning of the platinum group elements and gold between silicate and sulphide magmas in the Munni Munni Complex, Western Australia. *Geochim. Cosmochim. Acta* **57**, 1277-1290.

_____ & CAMPBELL, I.H. (1988): Role of late magmatic fluids in Merensky-type platinum deposits: a discussion. *Geology* **16**, 488-491.

BIRD, D.K., ARNASON, J.G., BRANDRISS, M.E., NEVLE, R.J., RADFORD, G., BERNSTEIN, S., GANNICOTT, R.A. & KELEMEN, P.B. (1995): A gold-bearing horizon in the Kap Edvard Holm complex, East Greenland. *Econ. Geol.* **90**, 1288-1300.

BORISOV, A. & PALME, H. (1997): Experimental determination of the solubility of platinum in silicate melts. *Geochim. Cosmochim. Acta* **61**, 4349-4357.

_____, _____ & SPETTEL, B. (1994): The solubility of Pd in silicate melts: implications for core formation in the Earth. *Geochim. Cosmochim. Acta* **58**, 705-716.

BOUDREAU, A.E. & MCCALLUM, I.S. (1992): Concentration of platinum-group elements by magmatic fluids in layered intrusions. *Econ. Geol.* **87**, 1830-1848.

_____ & MEURER, W.P. (1999): Chromatographic separation of the platinum-group elements, gold, base metals and sulfur during degassing of a compacting and solidifying igneous crystal pile. *Contrib. Mineral. Petrol.* **134**, 174-185.

_____, STEWART, M.A. & SPIVACK, A.J. (1997): Stable Cl-isotopes and origin of high-Cl magmas of the Stillwater Complex, Montana. *Geology* **25**, 791-794.

CAMPBELL, I.H., NALDRETT, A.J. & BARNES, S.J. (1983): A model for the origin of the platinum-rich sulphide horizons in the Bushveld and Stillwater complexes. *J. Petrol.* **24**, 33-165.

CARROLL, M.R. & WEBSTER, J.D. (1994): Solubilities of sulfur, noble gases, nitrogen, chlorine, and fluorine in magmas. *In* Volatiles in Magmas (M.R. Carroll & J.R. Holloway, eds.). *Rev. Mineral.* **30**, 231-279.

HOATSON, D.M. & KEAYS, R.R. (1989): Formation of platiniferous sulfide horizons by crystal fractionation and magma mixing in the Munni Munni layered intrusion, West Pilbara Block, Western Australia. *Econ. Geol.* **84**, 1775-1804.

HOLLAND, H.D. (1972): Granites, solutions and base metal deposits. *Econ. Geol.* **67**, 281-301.

HOLLOWAY, J.R. & BLANK, J.G. (1994): Application of experimental results to C–O–H species in natural melts. *In* Volatiles and Magmas (M.R. Carroll & J.R. Holloway, eds.). *Rev. Mineral.* **30**, 187-230.

HSU, L.C., LECHER, P.J. & NELSON, J.H. (1991): Hydrothermal solubility of palladium in chloride solutions from 300° to 700°C: preliminary experimental results. *Econ. Geol.* **86**, 422-427.

MCKENZIE, D. (1984): The generation and compaction of partially molten rock. *J. Petrol.* **25**, 713-765.

OBERTHÜR, T., WEISER, T.W. & KOJONEN, K. (2002): Local variations and regional trends in PGE geochemistry and mineralogy in the Main Sulfide Zone of the Great Dyke, Zimbabwe. *In* 9th Int. Platinum Symp. (Billings), Extended Abstr., 337-340.

PEACH, C.L. & MATHEZ, E.A. (1996): Constraints on the formation of platinum-group element deposits in igneous rocks. *Econ. Geol.* **91**, 439-450.

PRENDERGAST, M.D. & WILSON, A.H. (1989): The Great Dyke of Zimbabwe. II. Mineralization and mineral deposits. In Magmatic Sulphides – The Zimbabwe Volume (M.D. Prendergast & M.J. Jones, eds.). Institution of Mining and Metallurgy, London, U.K. (21-41).

SASSANI, D.C. & SHOCK, E.L. (1990): Speciation and solubility of palladium in aqueous magmatic–hydrothermal solutions. *Geology* **18**, 925-928.

SHI, PINGFANG (1992): Fluid fugacities and phase equilibria in the Fe–Si–O–H–S system. *Am. Mineral.* **77**, 1050-1066.

SHIRLEY, D.N. (1986): Compaction of igneous cumulates. *J. Geol.* **94**, 795-809.

SOBOLEV, A.V. & CHAUSSIDON, M. (1996): H_2O concentrations in primary melts from supra-subduction zones and mid-ocean ridges: implications for H_2O storage and recycling in the mantle. *Earth Planet. Sci. Lett.* **137**, 45-55.

VON ROSENBERG, D.U. (1969): *Methods for the Numerical Solution of Partial Differential Equations.* Elsevier, New York, N.Y.